

RESEARCH ARTICLE

ELECTROCHEMISTRY

Scalable and safe synthetic organic electroreduction inspired by Li-ion battery chemistry

Byron K. Peters^{1*}, Kevin X. Rodriguez^{1*}, Solomon H. Reisberg¹, Sebastian B. Beil¹, David P. Hickey², Yu Kawamata¹, Michael Collins³, Jeremy Starr³, Longrui Chen⁴, Sagar Udyavara⁵, Kevin Klunder², Timothy J. Gorey², Scott L. Anderson², Matthew Neurock^{5,†}, Shelley D. Minteer^{2,†}, Phil S. Baran^{1,†}

Reductive electrosynthesis has faced long-standing challenges in applications to complex organic substrates at scale. Here, we show how decades of research in lithium-ion battery materials, electrolytes, and additives can serve as an inspiration for achieving practically scalable reductive electrosynthetic conditions for the Birch reduction. Specifically, we demonstrate that using a sacrificial anode material (magnesium or aluminum), combined with a cheap, nontoxic, and water-soluble proton source (dimethylurea), and an overcharge protectant inspired by battery technology [tris(pyrrolidino)phosphoramidate] can allow for multigram-scale synthesis of pharmaceutically relevant building blocks. We show how these conditions have a very high level of functional-group tolerance relative to classical electrochemical and chemical dissolving-metal reductions. Finally, we demonstrate that the same electrochemical conditions can be applied to other dissolving metal-type reductive transformations, including McMurry couplings, reductive ketone deoxygenations, and epoxide openings.

The use of alkali metals as reagents for strongly reductive chemistry has been limited in the modern era owing to safety considerations and immense difficulty in industrial scale-up. The Birch reduction, a flagship example, is one of the first reactions taught in undergraduate organic chemistry lectures (1) for the rapid access it affords to sp³ complexity from simple feedstock arenes (2–5). Yet typical procedures call for the hazardous condensation of ammonia or other volatile amines as solvent, combined with pyrophoric metals at cryogenic temperatures. Milder alternatives have been reported that rely on finely dispersed silica-impregnated Na (SiGNa-SI) and Na/K (6–8) or various mineral oil dispersions combined with super-stoichiometric amounts of an expensive and toxic crown ether additive (9, 10). However, these reagents either fail to access the same reactivity space as, for example, Li/NH₃, or still require extreme caution in reaction setup on ac-

count of the alkali metal. Perhaps the most compelling modern Birch application stems from Pfizer's kilogram-scale synthesis of the anti-Parkinson's drug candidate sumanirole (2) (Fig. 1A) (11). The tandem aziridine opening and debenzoylation of the direct precursor 1 is a noteworthy achievement in process chemistry and engineering; it required the use of custom equipment to administer lithium metal, as well as enough ammonia to fill three Boeing 747 airliners in the gas phase. At the end of the reaction, which was conducted at cryogenic temperature (–35°C), 2300 liters of H₂ were liberated—an understandably intimidating occurrence.

In this context, electrochemical reduction is an appealing alternative. Indeed, several groups have explored the idea of electrochemical surrogates for alkali metal reductions (Fig. 1, B and C) (12–14), with a key report by Kashimura and co-workers demonstrating proof of concept for electrochemically driven Birch reactivity (15). Nonetheless, electrochemical reductions have been hindered by a myriad of unwanted side reactions that typically overpower the desired reactivity, including competing proton reduction, electrode passivation from excessive electrolysis of solvent, and diminished yields caused by adventitious O₂. Perhaps most telling is the fact that to synthesize 2 on process scale, Pfizer used chemical Birch reduction rather than any then-known electrochemical alternatives. For Pfizer, a kilogram-scale chemical Birch reduction was more practical to scale than any electrochem-

ical method, despite the enormous engineering challenges associated with the former. Corroborating these limitations, our attempts to reduce 1 using a variety of the known electrochemical conditions were completely fruitless (see supplementary materials).

Concurrent with these initial forays into electrochemical reduction, the quest to achieve a cyclable, safe, and high-energy density lithium-ion (Li-ion) battery has faced similar challenges, culminating in a better understanding of the role that additives, solvent, and electrolyte play in the formation of a solid electrolyte interphase (SEI) (16, 17). Importantly, the SEI prevents buildup of an excessive passivating layer at the electrode while enabling a more active and stable electrode interface under extreme potentials (Fig. 1D) (18, 19). Application of these concepts to Li-ion battery technology is largely responsible for their widespread use in virtually all modern electronics, including smartphones, laptops, and electric vehicles. Inspired by this transformative technology, we sought to optimize electro-organic synthesis using the approaches originally developed for Li-ion batteries (20). Here, we show that such strongly reducing conditions can be accessed in a simple and safe way, at ambient temperature without rigorous exclusion of air or moisture, and can be applied to the most popular reaction classes in this arena, such as Birch, debenzoylation, epoxide/aziridine opening, and McMurry couplings.

Electrochemistry represents a convenient way to precisely select redox potentials for use in organic synthesis. Anodic, or oxidative, processes constitute the vast majority of commonly employed electrochemical transformations and run the gamut of C–H oxidation (21), decarboxylation (22), oxidative couplings (23, 24), and olefin functionalizations (25, 26). In contrast, cathodic reductions (27–29) have been used considerably less in modern preparative synthesis. This lower utility is likely due to three factors: First, many reductive methods are limited to divided cells, which can seem daunting enough to frighten off prospective users, in addition to the engineering challenges they pose in setting up high-throughput screenings and scale-up contexts. (Note that divided cells are vitally important to preparative electrosynthesis, as they often alleviate redox incompatibilities and mismatches incurred in undivided cells, but with their complex construction, adoption from the broader synthetic community has been limited.) Second, most electroreductive methods rely on a mercury pool cathode, a technique with extreme health and safety repercussions. Finally, although there are examples of other reductive electrosyntheses in the literature that demonstrate good chemoselectivity under such reductive conditions (30), achieving chemoselectivity for electrochemical Birch reduction in the presence of other electrophores has remained an unmet challenge. Indeed, on approach of strongly reductive conditions (including those required to access Li⁰), most common electrolytes disintegrate (31, 32). Thus, although accessing this extreme reactivity using

¹Department of Chemistry, Scripps Research, La Jolla, CA 92037, USA. ²Department of Chemistry, University of Utah, Salt Lake City, UT 84112, USA. ³Discovery Sciences, Medicine Design, Pfizer Global Research and Development, Groton, CT 06340, USA. ⁴Asymchem Life Science (Tianjin), Tianjin Economic-Technological Development Zone, Tianjin 300457, China. ⁵Department of Chemical Engineering and Materials Science, University of Minnesota, Minneapolis, MN 55455, USA.

*These authors contributed equally to this work.

†Corresponding author. Email: pbaran@scripps.edu (P.S.B.); minteer@chem.utah.edu (S.D.M.); mneurock@umn.edu (M.N.)

cathodic reduction is not a new idea, accessing it in a way that is both practical and scalable is a goal that has not been achieved. Birch himself reported the first electrochemically mediated arene reduction of toluene (with NaOEt/NH₃) (33). Additional reports following up on that pioneering study have appeared, including the key report by Kashimura and co-workers (vide supra and Fig. 1C). However, all of these reports exhibit narrow scope—Kashimura’s method is limited to hydrocarbons—and they require procedures (e.g., continuous sonication) that are not

more scalable than a purely chemical Birch reduction (12, 13, 15, 34–47).

Li-ion battery interphase design applied to electroreduction

Accordingly, the current study began with an extensive evaluation of this prior art, of which select efforts are summarized in entries 1 to 4 of Fig. 1E (see supplementary materials for a complete listing) (12, 13, 15, 36, 42, 43, 48). To help probe the functional-group tolerance of these previous works, we opted for phenyl ethanol (**3**)

as a model substrate. The conditions reported by Kashimura and colleagues (15) were chosen as a basis from which to launch more extensive optimization (entry 4); however, the limitations of that state-of-the-art method were clearly demonstrated by the fact that the alcohol moiety of **3** completely shut down reactivity under Kashimura’s conditions. To optimize, LiClO₄ was first replaced with LiBr because of the bromide salt’s higher stability, affordability, and similar range of solubility; however, only trace product was detected (entry 5). An accumulation of an

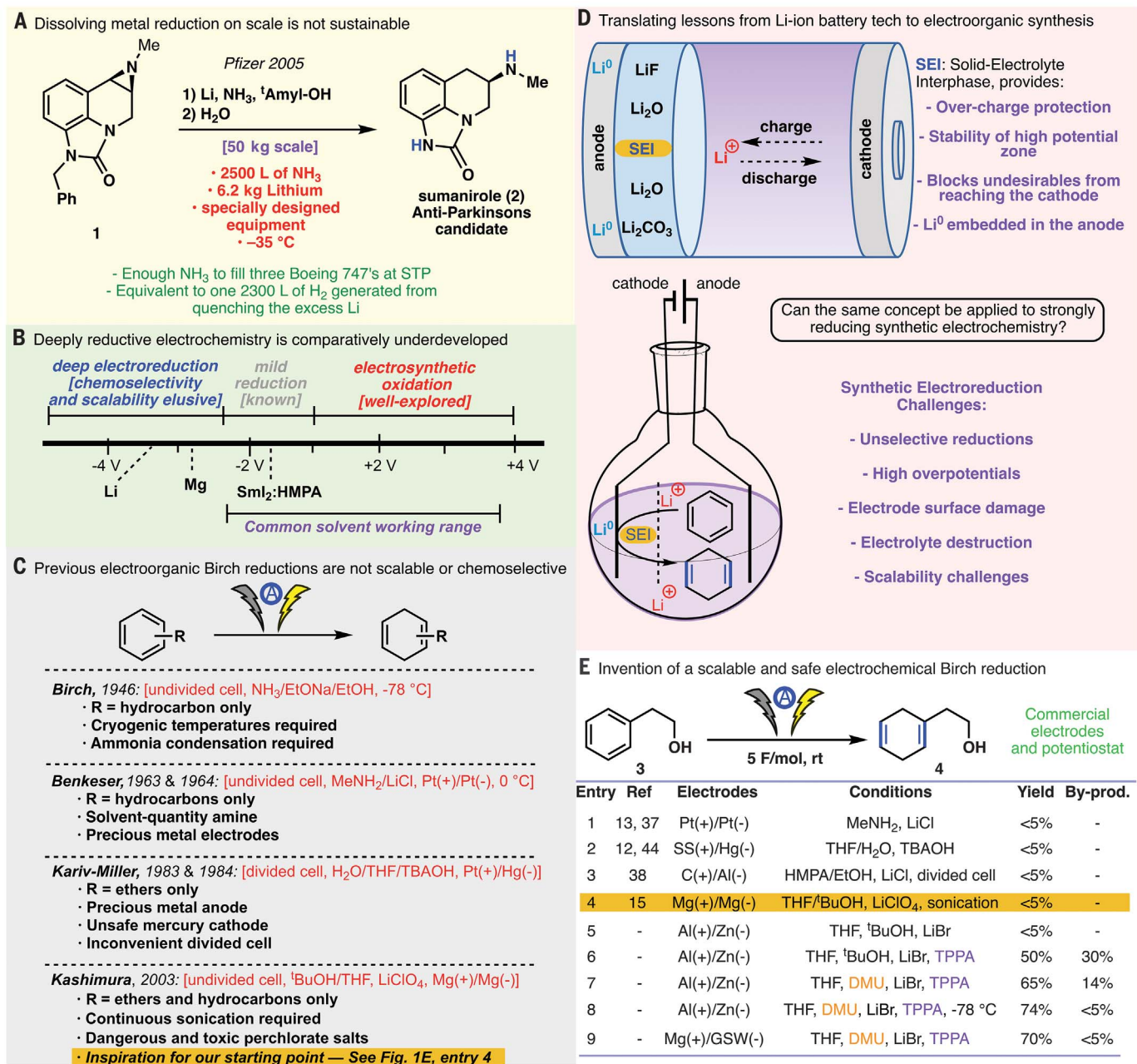


Fig. 1. Background and reaction development. (A) Dissolving metal reduction on scale is not sustainable. Me, methyl; Ph, phenyl; ^tAmyl, *tert*-amyl; STP, standard temperature and pressure. (B) Voltage range challenges for reductive electrochemistry. (C) Electrochemical

Birch precedence. Et, ethyl. (D) Applying Li-ion battery technology to synthetic electrochemistry. (E) Optimization of a simple electrochemical alternative to Birch reduction. TBAOH, tetrabutylammonium hydroxide; ^tBu, *tert*-butyl; GSW, galvanized steel wire.

apparently metallic substance at the cathode reacted violently with MeOH and water during cleaning, thus providing an initial clue for further study. We reasoned that this material was Li metal that had reductively plated out owing to the poor solubility of Li^0 in tetrahydrofuran (THF). Indeed, similar events were observed in the early days of Li-ion battery exploration as a result of battery overcharging (49). To combat this problem, several additives similar to those known for dampening the effects of overcharging in Li-ion batteries (including glyme, dioxane, and phosphoramidates; see supplementary materials for complete list) were evaluated, with tris(pyrrolidino)phosphoramidate (TPPA), a non-carcinogenic surrogate for hexamethylphosphoramide (HMPA) (50), emerging as optimal (entry 6). Although the desired product was observed in 50% yield, it was accompanied by undesired isomers and over-reduced species in ~30% yield. Unsurprisingly, varying the proton source had a profound effect on the distribution of these compounds. After an extensive screen (see supplementary materials), we determined that 1,3-dimethylurea (DMU) was the most selective for the desired product (entry 7). As expected, reduced temperature afforded greater selectivity (entry 8). Consistent with Kashimura's findings (15), it was found that switching from an Al to a Mg anode and increasing the current density on the cathode (by decreasing its surface area) rendered the reaction more selective and efficient at room temperature (entry 9). It is postulated that the anode is sacrificially oxidized, and it is possible that the identity of the resultant oxidized metal salts is relevant to the observed reactivity (vide infra).

Mechanistic investigation Electroanalytical and computational study of reaction kinetics

With an optimized set of conditions in hand, the mechanism of transformation was explored in a variety of contexts. Intuitively, one may assume that the cathode simply generates Li^0 species (whether homogeneous, heterogeneous, or electroplated) that are responsible for the observed reactivity, which in turn implies that electrolysis could be decoupled from the actual substrate reduction. To test this hypothesis, a degassed reaction solution—with the substrate and DMU omitted—was electrolyzed as normal, under an inert atmosphere at -78°C , to putatively accumulate electrochemically generated Li^0 species (51). After electrolysis was completed (1.5 hours, 5 F/mol), the substrate was added and the reaction was stirred, with samples drawn at 30-min intervals (Fig. 2A). There was a small decrease in the substrate concentration over time, but no desired product or well-defined side products could be detected during this time. Similar trends held true for an analogous experiment run at room temperature (see supplementary materials). The apparent disconnect between putative Li^0 generation and lack of Birch reactivity strongly suggested that a typical Li^0 species is not the active reductant in our reaction

manifold. We hypothesized that, instead, arene substrate was getting reduced directly on the electrode surface. To probe this hypothesis, we performed a variety of computational and electroanalytical experiments.

First, ab initio calculations (see supplementary materials for detailed methods) were undertaken (Fig. 2B) to compare the kinetics of the solution-phase reduction of **3** via Li^0 species (red path, top) to the kinetics of the direct reduction of **3** at the electrode surface at -2.25 V versus normal hydrogen electrode (NHE) (blue path, bottom). The reduction of **3** via the Li-mediated path is predicted to proceed initially via electron transfer from the lithium metal (Li^0) to **3**, forming the anion radical **3a** and generating the lithium cation (Li^+); **3a** is then protonated in the solution phase via DMU to form the radical intermediate (**3b**). This first protonation step, as shown in Fig. 2B, is the highest energy state along the path with an activation barrier of 52 kJ/mol. On the other hand, the electrode-mediated pathway began with the adsorption of **3** to the cathode, followed by an electron transfer event from the cathode, to generate adsorbed radical anion (**3a^{ads}**). Both adsorption and the heterogeneous electron transfer were calculated to be barrierless. Facile protonation of **3a^{ads}** resulted in the formation of the adsorbed radical **3b^{ads}**, which could undergo a second barrierless electrode-to-substrate electron transfer to produce the adsorbed anion (**3c^{ads}**). Finally, the rate-determining protonation gave the adsorbed diene **4^{ads}** with a calculated barrier of 41 kJ/mol. Facile desorption was calculated to give the solution-phase product (**4**). Comparing the two pathways, these computations clearly support superior kinetic facility of an on-electrode reductive mechanism rather than one mediated by Li^0 .

To further investigate reaction kinetics, the reaction was monitored [via gas chromatography-mass spectrometry (GC-MS) analysis of quenched aliquots] under standard electrochemical conditions at 5-min intervals (Fig. 2C, left). Essentially no induction period was observed, and no competitive processes were detected based on the absence of side products. Furthermore, analysis suggests zero-order kinetics in substrate: Consumption of phenyl ethanol **3** and formation of product were both well fitted by linear regression [coefficient of determination (R^2) = 0.99 and 0.98, respectively]. The slight deviation from linearity observed is likely due to the small dataset collected. We also studied the reaction rate's dependence on current (Fig. 2C, right). A clear positive correlation between current and rate was observed; we attempted to determine the rate order via Jordi-Burés plot (52). Although a first-order plot was the closest fit to the data (Fig. 2C, right inset), the fit was not perfect, suggesting that the rate's dependence on current is quite complex. Nonetheless, the rate order is clearly positive. Taken together, these data are consistent with a kinetic picture in which electron flow from the cathode, rather than any chemical transformation, is rate-limiting.

Although voltammetric studies on the electrochemical reduction of arenes have been performed by others, the focus of these studies was on polyaromatics as electron shuttles, mediators, or catalysts rather than as substrates, and they therefore did not elucidate the details of protonation and second electron transfer events (53). We thus set out to study the microscopic electrochemical steps using a combination of voltammetric techniques (Fig. 3). We initially hoped to use **3** as a model. Unfortunately, under very similar conditions to our preparative reduction, lithium alkoxides are electrochemically generated at potentials higher (less negative) than that of **3**, thereby obfuscating critical details of the electron transfer steps. Under the general assumption that a given mechanism (or set of mechanisms) is common to all substrates, our focus shifted to naphthalene (**5**) as a model substrate for voltammetric analysis under our optimized reaction conditions. Square wave voltammetry (SWV) of **5** (Fig. 3A) indicated two distinguishable electrochemical reduction steps that are resolved at high frequencies [i.e., some electron transfer, electron transfer (EE) process]. This result is consistent with a mechanism involving direct reduction of **5** at the electrode. It should be noted that this two-electron transfer could occur either consecutively, before two subsequent protonation steps [electron transfer, electron transfer, chemical protonation, chemical protonation (EECC) mechanism], or with a chemical step separating them [electron transfer, chemical protonation, electron transfer, chemical protonation (ECEC) mechanism]. To differentiate between these possibilities, we used cyclic voltammetry (CV) (see supplementary materials), the results of which revealed that varying the CV potential window had an influence on the reversibility of the scan. This is inconsistent with an EE mechanism and demonstrates that these two processes are separated by a chemical step (protonation), prompting us to invoke an ECEC mechanism (refer to supplementary materials for in-depth discussion). Although elements of the data are also consistent with an electrochemical disproportionation (DISP)-type mechanism, the zero-order kinetics in substrate (vide supra) is not. Thus, an ECEC-type mechanism seems most likely.

These CV experiments also demonstrated that without LiBr, the scans showed good reversibility, highlighting the crucial role of Li^+ in guiding the reaction toward the product. Combining this insight with DMU's superiority as a proton donor (see supplementary materials for other proton sources screened), we probed the possible interaction between Li^+ and DMU via attenuated total reflectance (ATR) (Fig. 3B). We observed a complete shift in the C=O stretching frequency of DMU from 1620 to 1660 cm^{-1} in the absence and presence of LiBr, respectively, which provides strong evidence for a Li^+ /DMU complexation.

All of these results are consistent with a mechanism involving sequential electrode-mediated single-electron reduction, protonation, additional

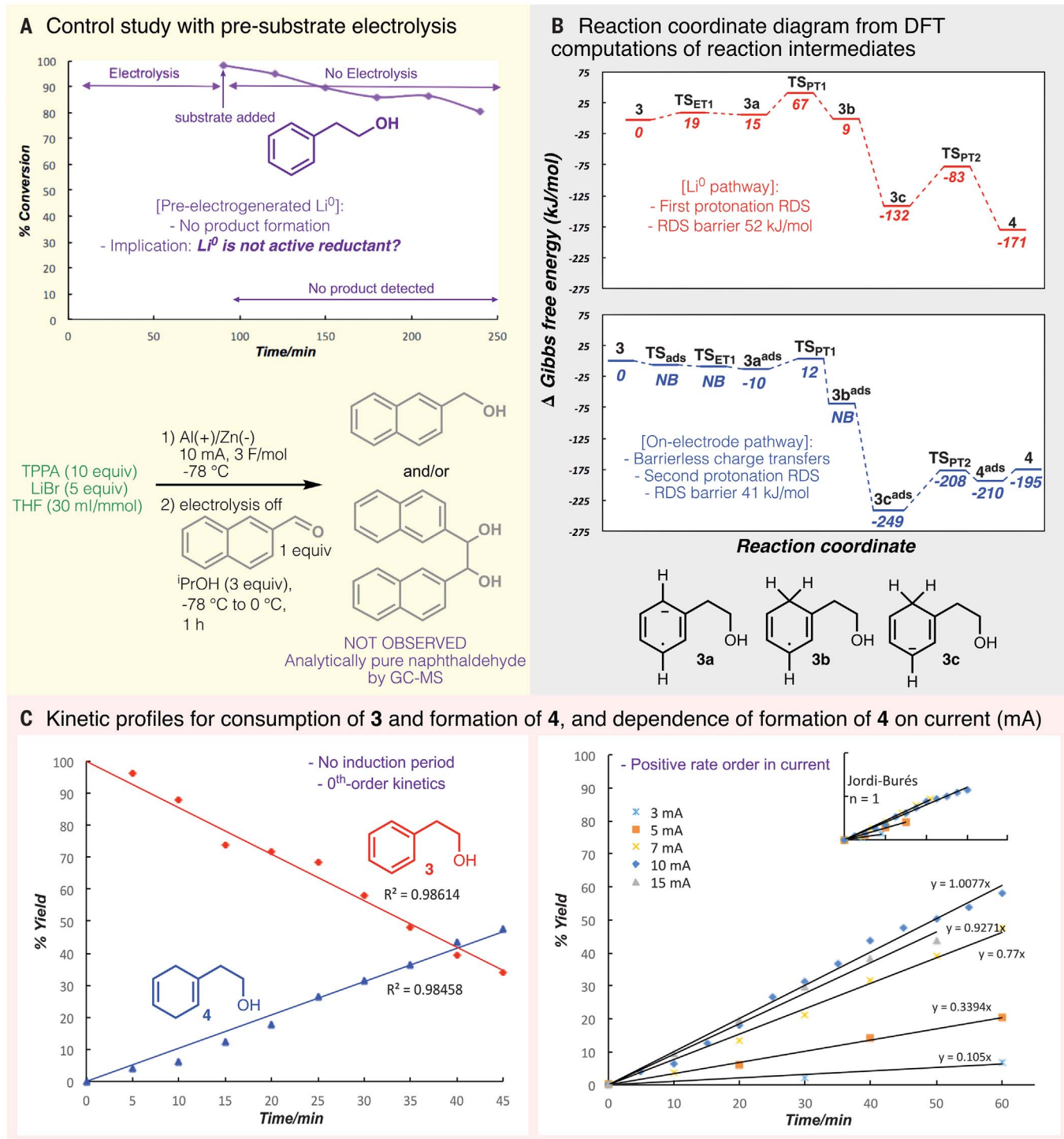


Fig. 2. Experimental and computational analysis of the electroreduction of phenyl ethanol (3). (A) Kinetic profile for the relative concentration of arene (3) in a control experiment involving pre-electrolysis of LiBr solution and Li^0 /solvated electron detection experiment with naphthaldehyde.

Pr , *iso*-propyl. (B) Reaction coordinate diagram from DFT computations of reaction intermediates for the reduction of 3 using either solution-phase Li^0 mediation as an electron source (red, top) or a heterogeneous zinc electrode at -2.25 V versus NHE as an electron source (blue, bottom). $\text{TS}_{\text{ET}1}$, transition state for electron transfer 1; $\text{TS}_{\text{PT}1}$,

transition state for proton transfer 1; $\text{TS}_{\text{PT}2}$, transition state for proton transfer 2; TS_{ads} , transition state for adsorption; NB, no barrier; RDS, rate-determining step; "ads" superscripts refer to adsorbed species.

(C) (Left) Plot of yield of 4 generated per time under the standard reaction conditions, indicating zero-order kinetics with respect to both the formation of 4 and consumption of 3. Final yield of 4 is 70%. (Right) Plot of yield of 4 generated per time under varying current. (Inset) Jordi-Burés analysis of current rate dependence, showing current dependence that approximates first-order kinetics.

electrode-mediated reduction, and a final protonation (Fig. 3C). The ability of Li^+ to form a relatively strong coordinative complex to DMU may be critical to localize DMU and the radical anion of **5** (Fig. 3D, top). To support this hypothesis for the role of Li^+ in the reaction manifold, we conducted control experiments with NaBr and KBr in place of LiBr. Although no reaction was observed, the inherent insolubility of these salts substantially altered the resistivity of the solution, thus thwarting direct comparisons to the LiBr system. Nonetheless, more soluble surrogates of these non-lithium cations, such as NaI, did not afford any product.

Regardless of the nuanced role of Li^+ in the reaction, these studies conclusively show that Li^0 does not play a role as a direct solution-phase

arene reductant. Furthermore, on treating a pre-electrolyzed LiBr solution (at -78°C) with a more reductively labile aldehyde, we did not observe any of the reduced alcohol or pinacol products (see Fig. 2A and supplementary materials). These data rule out the mechanistic possibility of solvated electrons as the active reductant. Preliminary investigations into the rate laws of the reaction show a complicated kinetic picture where multiple pathways may be operative; more detailed studies on the mechanism and kinetics of this reaction manifold are ongoing in our laboratories.

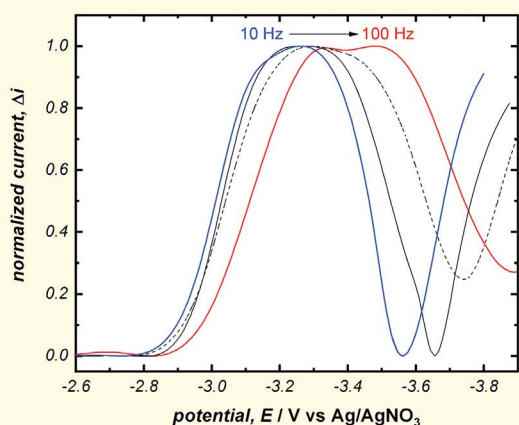
Electrode surface interrogation

The addition of TPPA to the **5**/DMU/LiBr solution does not result in the increased electron

transfer rates that would be expected of electrochemical mediation through $\text{Li}^{+/0}$. This suggests that the role of TPPA may not be intrinsically tied to the mechanistic cycle but instead may be involved in ancillary electrochemical processes (Fig. 3C). Structurally similar molecules (such as HMPA) have been employed in Li-ion batteries to aid in dissolving Li_2O layers formed at the electrode interface (54). With this in mind, the speciation at the electrode surface was investigated using x-ray photoelectron spectroscopy (XPS).

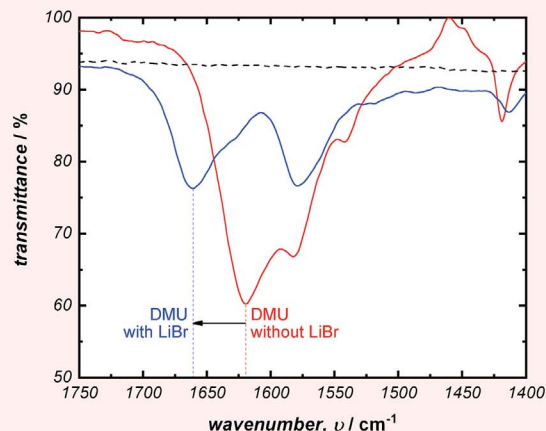
In general, a major problem with electroorganic synthesis under extreme reductive potentials is the formation of thick passivation layers on the electrode surface that inhibit product formation and lead to extensive side products. Evidence of this passivation in our system

A Variable-frequency square wave voltammetry of **5**



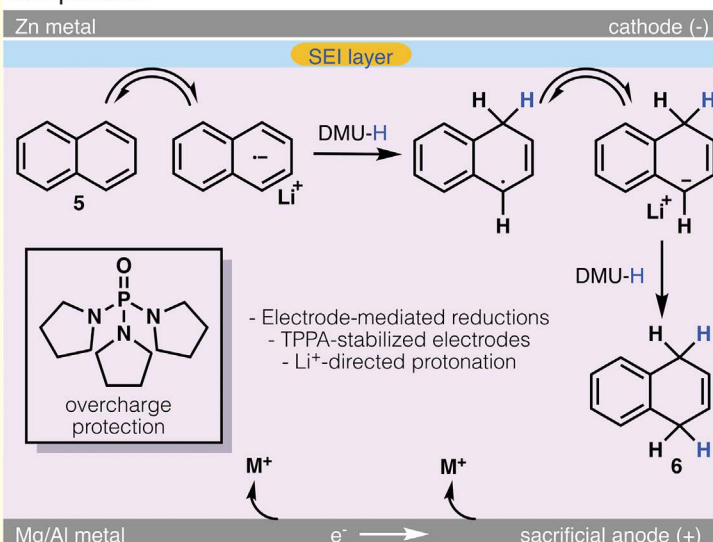
- [At high frequency]: Two distinct reductive waves
- Implication: Two unique reductions; not 2X Li^+ reduction

B ATR IR of DMU with/without LiBr



- C=O vibrational shift with LiBr
- Implication: Li^+ /DMU complexation

C Proposed mechanism based on voltammetry and computation



D Proposed intermediate preceding protonation

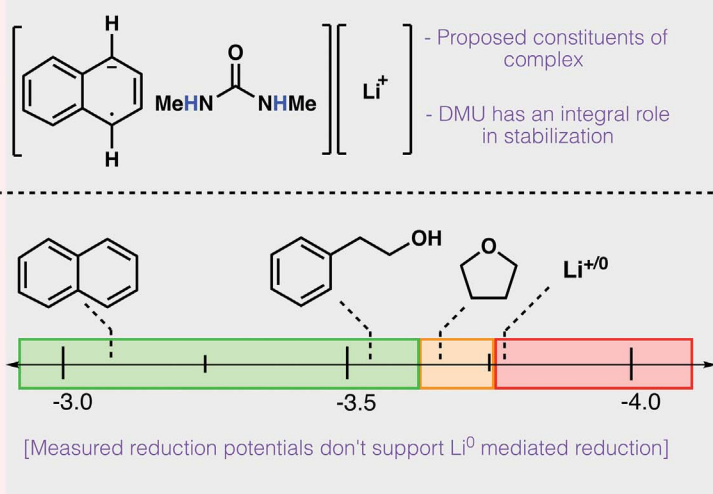


Fig. 3. Electrochemical data used to determine the role of various reaction components. (A) Comparative SWVs of 1 mM naphthalene (**5**) at 10 Hz (blue) and 100 Hz (red). (B) ATR-infrared (IR) spectrum of DMU with and without LiBr (blue and red, respectively). (C) Scheme of the proposed mechanism of electrochemical Birch reduction. (D) Proposed intermediate preceding the protonation.

was demonstrated in the absence of TPPA, as shown in the supplementary materials. Although optimized conditions still evidenced a thin film on the electrode surface (see supplementary materials), this film ceased to grow within minutes and appeared to stabilize along the working electrode. XPS analysis revealed Mg, P, N, and large amounts of lithium deposited on the electrode surface, as well as increased levels of oxygen and carbon; detailed analysis of the spectra is provided in the supplementary materials. The observed Li, O, and C are likely a result of THF decomposition to form Li alkox-

ide (55). Surprisingly, zinc was still observed in the postreaction film, providing evidence that the underlying electrode material is still accessible to the bulk solution. The film may also be involved in both forming a stable SEI and providing an active electrode surface for the reaction. Although the exact mechanisms of film growth and suppression are not yet known, it is clear that all system components are incorporated into the film and may cooperatively maintain electrode activity.

Finally, given our use of a sacrificial anode and its putative generation of magnesium salts

during the reaction, we also probed the possible role of anode-derived magnesium salts in the reaction mechanism. We found that addition of stoichiometric and super-stoichiometric amounts of $\text{MgBr}_2 \cdot \text{Et}_2\text{O}$ under our electrochemical protocol not only gave the desired diene **4** in a diminished yield (30% versus 74%) but also gave an overall lower consumption of **3** (see supplementary materials). In addition, we observed that, in the absence of stirring, diminished yields could be correlated with decreased distances between the cathode and anode, suggesting that diffusion of metal salts from the anode is

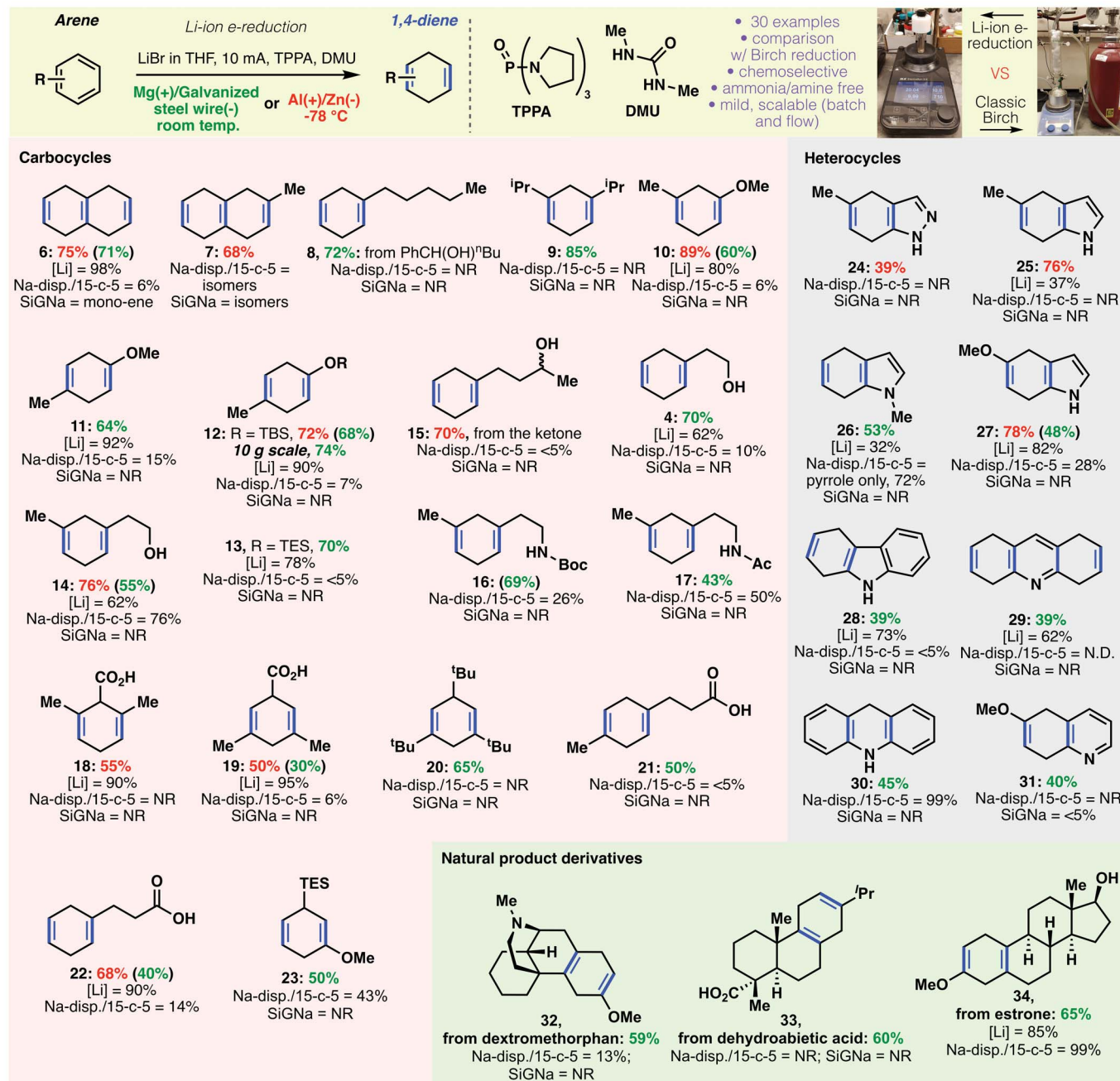


Fig. 4. Scope of the electrochemical Birch reaction, encompassing arenes and heterocycles, and comparison to other modern Birch alternatives. NR, no reaction.

deleterious to the reaction. Although we cannot fully rule out that these metallic ions are mechanistically relevant, given the deleterious nature of Mg salts to the overall reaction, we hypothesize that any exogenous salts generated under the electrochemical conditions are most likely not mechanistically critical.

Applications to complex substrates

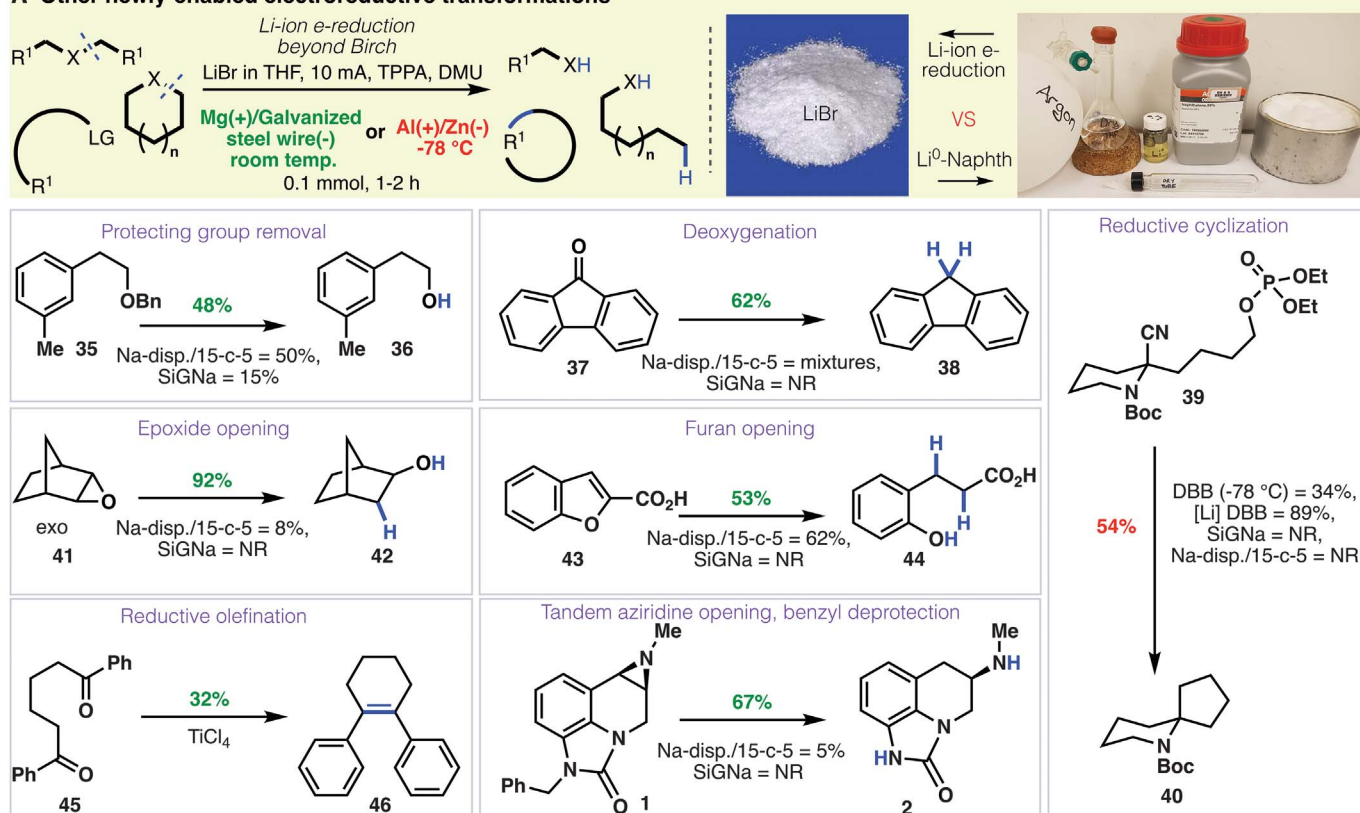
As shown in Fig. 4, the electroreduction exhibited a broad scope across a range of different arenes. Under optimized conditions, every aryl group within a given polyarene was efficiently reduced (**6** and **7**)—an achievement not accomplished by ammonia-free variants (e.g., SiGNa) (**8**), other dispersions (**10**), or more weakly reduc-

tive conditions (**56**). Simple arenes proved facile (**8** and **9**), as did aryl ethers, including those with both meta and para substituents (**10** and **11**). Silyl ethers performed well (**12** and **13**), despite their conspicuous absence from other ammonia-free alternatives. The utility of these modular intermediates is evident from the large body of literature in which they appear (**57**). Consistent with reactivity of the classical Birch, alcohol and ketone-containing arenes (**4**, **14**, and **15**) were reduced in good yields (accompanied by the anticipated ketone reduction). Carbamate (**16**), amide (**17**), carboxylic acid (**18**, **19**, **21**, and **22**), and silane (**23**) functionalities were also preserved in the reduction of the aryl group. Even a sterically guarded substrate, 1,3,5-tri-*tert*-butylbenzene, could

be reduced efficiently (**20**). Benzoic acids were furnished in moderate yields (**18** and **19**); to our knowledge, this substrate class has historically been restricted to standard Birch conditions. The operational simplicity of this chemistry is displayed in the Birch reduction of substrate **3**; when no precautions were taken to exclude air or moisture, the reaction resulted in a similar conversion (68%).

Heterocyclic arenes, which are rarely subjected to Birch reductions, proved viable substrates. Indazole (**24**), indole (**25**, **26**, and **27**), carbazole (**28**), acridine (**29** and **30**), and quinoline (**31**) moieties could be reduced on the carbocyclic ring in preference to the heterocycle, a reactivity only possible under a few classic Birch

A Other newly-enabled electroreductive transformations



B Modular scalability of electrochemical Birch in flow

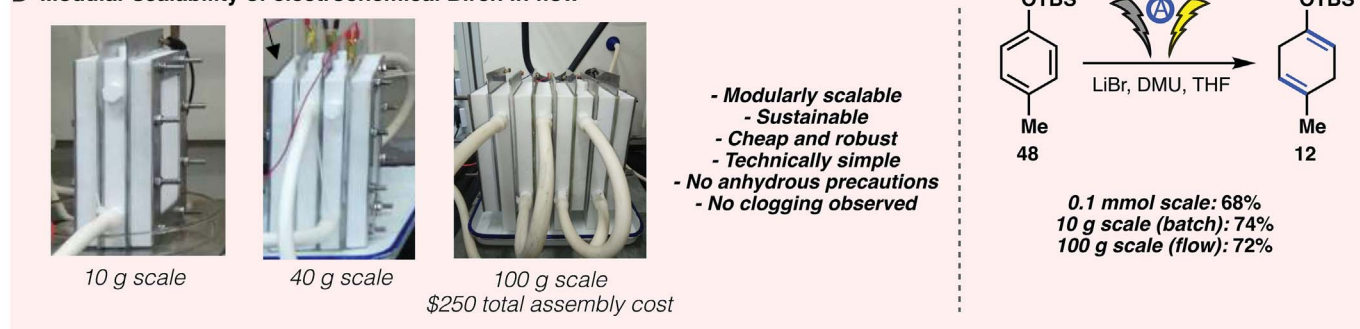


Fig. 5. Scope of other reductive electro-organic transformations. (A) Scope of the electrochemical reduction in a variety of other reactions. R¹, alkyl or aryl; X, halide or pseudohalide; LG, leaving group; Boc, butoxycarbonyl; DBB, di-*tert*-butylbiphenyl. (B) Modular scale-up of Birch reduction in flow. OTBS, *tert*-butyldimethylsilyloxy.

conditions. SiGNa-S1 failed in all the examples tested (Fig. 4), and Na-dispersion/15-crown-5 (Na-disp./15-c-5) mixture gave only partial conversion with prolonged reaction times on some substrates.

The mildness of the reaction conditions was demonstrated via application to more complex natural products. Thus, chemo- and regioselective reduction gave access to the 1,4-dienyl derivatives of dextromethorphan (**32**), dehydroabiatic acid (**33**), and estrone methyl ether (**34**). Overall, this methodology was competitive to the chemical Birch using lithium metal (see supplementary materials for the referenced literature comparisons).

More broadly, the chemistry of dissolving metals has been applied to a wide range of reductive transformations, including ring opening and closing (**58**), protecting group removal, and transition metal-mediated reactions, among others. However, because of the poor solubility of alkali metals in reductively inert solvents (e.g., THF), these reactions have required either the use of ammonia as a cosolvent or the aid of polyaromatic hydrocarbons to act as electron shuttles (**59**). In contrast, generation of reductive potential can be precisely controlled in electrochemical systems; as a result, the limitations associated with bulk Li metal are eliminated. Encouraged by this realization, we began to explore the utility of our electroreduction protocol for non-Birch reductive transformations (Fig. 5A). Ether debenzoylation proceeded smoothly (**35**→**36**) without competitive reduction of the more electron-rich arene (in accord with Birch guidelines). Similarly, reductive deoxygenation was accomplished on fluorenone (**37**→**38**). Reductive cyclization (**39**→**40**), similar to an approach demonstrated by Wolckenhauer and Rychnovsky (**60**), was successfully achieved. Ring opening of an epoxide (**41**→**42**) was facile, as was furan ring opening (**43**→**44**). Remarkably, McMurry couplings (**45**→**46**) could also be accomplished at room temperature. Returning to the sumanirole example outlined in Fig. 1, the same transformation was readily achieved at room temperature in 2 hours (**1**→**2**, 67% yield). It is worth noting that the most practical Birch alternatives available (SiGNa-S1 and Na-disp./15-c-5) failed to deliver any product, as did all attempts to use previously reported electrochemical methods (see supplementary materials).

Finally, the scalability of the protocol was demonstrated in both batch and flow on **12** (the direct precursor to a key Pfizer intermediate), without any loss in efficiency. The modular flow setup (Fig. 5B) is simple and allows an increase in scale by several orders of magnitude in a safe and sustainable fashion. Indeed, the very same transformation could be achieved in flow on 100-g scale, without major changes to the protocol, special anhydrous precautions, or loss in yield.

Reductive electrochemical synthesis has been an approach discussed in the literature for nearly a century. Despite its obvious conceptual appeal, adoption of preparative methods in this subfield has been extremely limited because of issues re-

lated to pragmatism and chemoselectivity. Inspired by Li-ion battery technology, we have developed a general set of electrochemical reductive conditions and demonstrated its practicality, safety, scalability, and chemoselectivity. We believe that inspiration from the fast-evolving research areas of battery technologies and electroactive materials will have an important impact in synthetic organic electrochemistry, in ways such as the discovery of new oxidative and reductive mediators, milder access to harsh reducing agents, and generation of low-valent catalytic systems based on transition metals.

REFERENCES AND NOTES

- P. W. Rabideau, Z. Marciniow, in *Organic Reactions, Volume 42*, L. A. Paquette, Ed. (Wiley, 1992), pp. 1–334.
- W. Rabten, C. Margarita, L. Eriksson, P. G. Andersson, *Chemistry* **24**, 1681–1685 (2018).
- B. K. Peters et al., *J. Am. Chem. Soc.* **138**, 11930–11935 (2016).
- J. Liu et al., *J. Am. Chem. Soc.* **139**, 14470–14475 (2017).
- A. Paptchikhine, K. Ilto, P. G. Andersson, *Chem. Commun.* **47**, 3989–3991 (2011).
- J. L. Dye et al., *J. Am. Chem. Soc.* **127**, 9338–9339 (2005).
- P. Nandi et al., *Org. Lett.* **10**, 5441–5444 (2008).
- M. J. Costanzo, M. N. Patel, K. A. Petersen, P. F. Vogt, *Tetrahedron Lett.* **50**, 5463–5466 (2009).
- P. Li, S. Guo, J. Fang, J. Cheng, *Huaxue Shiji* **18**, 234–236 (1996).
- P. Lei et al., *Org. Lett.* **20**, 3439–3442 (2018).
- D. K. Joshi, J. W. Sutton, S. Carver, J. P. Blanchard, *Org. Process Res. Dev.* **9**, 997–1002 (2005).
- K. E. Swenson, D. Zemach, C. Nanjundiah, E. Kariv-Miller, *J. Org. Chem.* **48**, 1777–1779 (1983).
- R. A. Benkeser, E. M. Kaiser, *J. Am. Chem. Soc.* **85**, 2858–2859 (1963).
- M. Bordeau, C. Biran, P. Pons, M. P. Leger-Lambert, J. Dunogues, *J. Org. Chem.* **57**, 4705–4711 (1992).
- M. Ishifune et al., *Electrochim. Acta* **48**, 2405–2409 (2003).
- J. B. Goodenough, K.-S. Park, *J. Am. Chem. Soc.* **135**, 1167–1176 (2013).
- J. B. Goodenough, Y. Kim, *Chem. Mater.* **22**, 587–603 (2010).
- E. Peled, S. Menkin, *J. Electrochem. Soc.* **164**, A1703–A1719 (2017).
- A. M. Haregewoin, A. S. Wotango, B.-J. Hwang, *Energy Environ. Sci.* **9**, 1955–1988 (2016).
- K. Mizushima, P. C. Jones, P. J. Wiseman, J. B. Goodenough, *Mater. Res. Bull.* **15**, 783–789 (1980).
- Y. Kawamata et al., *J. Am. Chem. Soc.* **139**, 7448–7451 (2017).
- S. Behr, K. Hegemann, H. Schimanski, R. Fröhlich, G. Haufe, *Eur. J. Org. Chem.* **2004**, 3884–3892 (2004).
- A. Kirste, B. Elsler, G. Schnakenburg, S. R. Waldvogel, *J. Am. Chem. Soc.* **134**, 3571–3576 (2012).
- J. Mihelcic, K. D. Moeller, *J. Am. Chem. Soc.* **126**, 9106–9111 (2004).
- Y. Ashikari, T. Nokami, J. Yoshida, *Org. Lett.* **14**, 938–941 (2012).
- T. Nokami et al., *J. Am. Chem. Soc.* **130**, 10864–10865 (2008).
- R. J. Perkins, D. J. Pedro, E. C. Hansen, *Org. Lett.* **19**, 3755–3758 (2017).
- G. Sun, S. Ren, X. Zhu, M. Huang, Y. Wan, *Org. Lett.* **18**, 544–547 (2016).
- C. Edinger, S. R. Waldvogel, *Eur. J. Org. Chem.* **2014**, 5144–5148 (2014).
- R. D. Little et al., *J. Org. Chem.* **53**, 2287–2294 (1988).
- J. Mortensen, J. Heinze, *Angew. Chem. Int. Ed. Engl.* **23**, 84–85 (1984).
- M. P. S. Mousavi, S. Kasefolgheta, A. Stein, P. Buhlmann, *J. Electrochem. Soc.* **163**, H74–H80 (2016).
- A. J. Birch, *Nature* **158**, 60 (1946).
- N. M. Alpatova, S. E. Zabusova, A. P. Tomilov, *Russ. Chem. Rev.* **55**, 99–112 (1986).
- H. W. Sternberg, R. Markby, I. Wender, *J. Electrochem. Soc.* **110**, 425–429 (1963).
- R. A. Benkeser, E. M. Kaiser, R. F. Lambert, *J. Am. Chem. Soc.* **86**, 5272–5276 (1964).

- H. W. Sternberg, R. E. Markby, I. Wender, D. M. Mohlner, *J. Am. Chem. Soc.* **89**, 186–187 (1967).
- A. Misono, T. Osa, T. Yamagishi, T. Kodama, *J. Electrochem. Soc.* **115**, 266–267 (1968).
- J.-E. Dubois, G. Dodin, *Tetrahedron Lett.* **10**, 2325–2328 (1969).
- L. A. Avaca, A. Bewick, *J. Chem. Soc. Perkin Trans. 2* **1972**, 1709–1712 (1972).
- J. P. Coleman, J. H. Wagenknecht, *J. Electrochem. Soc.* **128**, 322–326 (1981).
- R. A. Misra, A. K. Yadav, *Bull. Chem. Soc. Jpn.* **55**, 347–348 (1982).
- E. Kariv-Miller, K. E. Swenson, D. Zemach, *J. Org. Chem.* **48**, 4210–4214 (1983).
- D. Pasquariello et al., *J. Phys. Chem.* **89**, 1243–1245 (1985).
- F. J. Del Campo et al., *J. Electroanal. Chem.* **507**, 144–151 (2001).
- C. Combellas, H. Marzouk, A. Thiebault, *J. Appl. Electrochem.* **21**, 267–275 (1991).
- P. J. M. van Andel-Scheffer, A. H. Wonders, E. Barendrecht, *J. Electroanal. Chem.* **366**, 143–146 (1994).
- Y. Landais, E. Zekri, *Eur. J. Org. Chem.* **2002**, 4037–4053 (2002).
- K. Liu, Y. Liu, D. Lin, A. Pei, Y. Cui, *Sci. Adv.* **4**, eaas9820 (2018).
- J. Coste, D. Le-Nguyen, B. Castro, *Tetrahedron Lett.* **31**, 205–208 (1990).
- C. A. Paddon, S. E. W. Jones, F. L. Bhatti, T. J. Donohoe, R. G. Compton, *J. Phys. Org. Chem.* **20**, 677–684 (2007).
- J. Burés, *Angew. Chem. Int. Ed.* **55**, 2028–2031 (2016).
- N. C. L. Wood, C. A. Paddon, F. L. Bhatti, T. J. Donohoe, R. G. Compton, *J. Phys. Org. Chem.* **20**, 732–742 (2007).
- B. Zhou et al., *Adv. Mater.* **29**, 1701568 (2017).
- O. (Youngman) Chusid, E. Ein Ely, D. Aurbach, M. Babai, Y. Carmeli, *J. Power Sources* **43**, 47–64 (1993).
- T. J. Donohoe, D. House, *J. Org. Chem.* **67**, 5015–5018 (2002).
- M. M. Heravi, M. V. Fard, Z. Faghghi, *Curr. Org. Chem.* **19**, 1491–1525 (2015).
- M. Yus, F. Foubelo, *Targets Heterocycl. Syst.* **6**, 136–171 (2002).
- R. Luisi, V. Capriati, Eds., *Lithium Compounds in Organic Synthesis: From Fundamentals to Applications* (Wiley-VCH, 2014).
- S. A. Wolckenhauer, S. D. Rychnovsky, *Org. Lett.* **6**, 2745–2748 (2004).

ACKNOWLEDGMENTS

We thank W. Qiao for assistance in setting up scale-up reactions. We also thank D. Blackmond for assistance in interpreting the kinetics data. **Funding:** Financial support for this work was provided by NSF (CCI Phase I grant 1740656) to M.N., S.D.M., and P.S.B. Financial support was also provided by Pfizer and Asymchem. B.K.P. and K.X.R. acknowledge the Swedish Research Council (Vetenskapsrådet, VR 2017-00362) and National Institutes of Health (PA-18-586), respectively, for funding their postdoc fellowships. Y.K. acknowledges the Hewitt Foundation for a postdoctoral fellowship. S.H.R. acknowledges an NSF GRFP (#2017237151) and a Donald and Delia Baxter Fellowship. **Author contributions:** B.K.P. and P.S.B. conceived of the project. B.K.P., K.X.R., S.H.R., S.B.B., D.P.H., Y.K., M.C., J.S., S.U., K.K., T.J.G., S.L.A., M.N., S.D.M., and P.S.B. designed the experiments. B.K.P., K.X.R., S.H.R., S.B.B., D.P.H., L.C., S.U., and K.K. ran the experiments. B.K.P., K.X.R., S.H.R., S.B.B., D.P.H., Y.K., M.C., J.S., S.U., K.K., T.J.G., S.L.A., M.N., S.D.M., and P.S.B. analyzed the data. B.K.P., K.X.R., S.H.R., D.P.H., S.U., M.N., S.D.M., and P.S.B. wrote the manuscript. **Competing interests:** P.S.B. serves on a scientific advisory panel for Asymchem. **Data and materials availability:** Detailed experimental and analytical procedures and full spectral data are available in the supplementary materials.

SUPPLEMENTARY MATERIALS

www.sciencemag.org/content/363/6429/838/suppl/DC1
Materials and Methods
Supplementary Text
Figs. S1 to S83
Tables S1 to S7
NMR Spectra
References (61–112)

28 September 2018; accepted 23 January 2019
10.1126/science.aav5606

Scalable and safe synthetic organic electroreduction inspired by Li-ion battery chemistry

Byron K. Peters, Kevin X. Rodriguez, Solomon H. Reisberg, Sebastian B. Beil, David P. Hickey, Yu Kawamata, Michael Collins, Jeremy Starr, Longrui Chen, Sagar Udyavara, Kevin Klunder, Timothy J. Gorey, Scott L. Anderson, Matthew Neurock, Shelley D. Minter and Phil S. Baran

Science **363** (6429), 838-845.
DOI: 10.1126/science.aav5606

Scaled-up sodium-free Birch reductions

The so-called Birch reduction is frequently used by chemists despite its daunting conditions: Pyrophoric sodium is dissolved in pure liquified ammonia to achieve partial reduction of aromatics. Peters *et al.* surveyed and then optimized small-scale electrochemical alternatives to devise a safer protocol that can work on a larger scale with a broad range of functionally complex substrates.

Science, this issue p. 838

ARTICLE TOOLS

<http://science.sciencemag.org/content/363/6429/838>

SUPPLEMENTARY MATERIALS

<http://science.sciencemag.org/content/suppl/2019/02/20/363.6429.838.DC1>

REFERENCES

This article cites 107 articles, 5 of which you can access for free
<http://science.sciencemag.org/content/363/6429/838#BIBL>

PERMISSIONS

<http://www.sciencemag.org/help/reprints-and-permissions>

Use of this article is subject to the [Terms of Service](#)